New Thermal Transitions in Stimuli-Responsive Copolymer Films

Fang Liu and Marek W. Urban*

Shelby F. Thames Polymer Science Research Center, School of Polymers and High Performance Materials, The University of Southern Mississippi, Hattiesburg, Mississippi 39406

Received October 14, 2008; Revised Manuscript Received January 9, 2009

ABSTRACT: These studies report for the first time new thermal relaxations in stimuli-responsive solid-phase copolymers detected by differential scanning calorimetry (DSC) and dynamic mechanical analysis (DMA). When 2-(*N*,*N*-dimethylamino)ethyl methacrylate (DMAEMA) and *n*-butyl acrylate (nBA) monomers were copolymerized into colloidal dispersions and allowed to coalesce to form solid continuous films, in addition to the glass-transition temperature (T_g), which follows the Fox equation for random copolymers, a new composition-sensitive endothermic stimuli-responsive transition (T_{SR}) was observed. The T_{SR} transition changes with the composition of the stimuli-responsive component of the copolymer, the temperature, and the rate of temperature change. On the basis of the experimental data, the following relationship was established: $1/T_{SR} = w_1/T_{binary} + w_2/T$ or $1/T_{SR} = w_1(1/T_{binary} - 1/T) + 1/T$, where T_{SR} is the temperature of the stimuli-responsive transition, T_{binary} is the temperature of the stimuli-responsive homopolymer in a binary polymer−water equilibrium, w_1 and w_2 ($w_2 = 1 - w_1$) are weight fractions of each component of the copolymer, and T is the film-formation temperature. This relationship allows us to predict T_{SR} transitions in stimuli-responsive solid copolymers. The enthalpic (ΔH) components of the T_g and T_{SR} transitions determined from DSC measurements are 122 kcal/mol for T_g and 199 kcal/mol for T_{SR}, which are part of the total energy, ΔE_{tot}, of the system. The calculated values of the ΔE_{tot} obtained using computer modeling simulations (168 kcal/mol for T_g and 223 kcal/mol for T_{SR}, respectively) are in good agreement with the experimental data, and the energy difference is attributed to the inclusion of the entropic components in ΔE_{tot} calculations.

Introduction

Whereas it is well established that polymers exhibit α, *β*, crystallization, and melting thermal relaxations, the presence of stimuli-responsive components, in particular those units that exhibit lower critical solution temperature (T_{LCST}) in solutions, may result in more complex thermal responses. Recently, we have reported[1] that poly((*N*-(DL)-(1-hydroxymethyl)propylmethyacrylamide/*n*-butyl acrylate) (p(DL-HMPMA/nBA)) solid films exhibit an 18.5% shrinkage in the 27−37 °C range, which results from the collapse of hydrophobic segments and buckling of the polymer backbone. These studies have also shown that to develop stimuli-responsive solid-state films, the presence of low-T_g (α transition) components, such as nBA (T_g of p(nBA) ≈ −46 °C),[1,2] may be required to facilitate the sufficient free volume that is necessary for remodeling of network components. Along the same theme, poly(2-(*N*,*N*-dimethylamino)ethyl methacrylate/*n*-butyl acrylate) (p(DMAEMA/nBA)) copolymer films were prepared and exhibit dual pH and temperature responsiveness.[3] These studies showed that solid p(DMAEMA/nBA) films also exhibit a 29.6% volume decrease[3] above an endothermic transition that is above the T_g of the copolymer. During the course of these studies, we noted that thermal transitions in continuous films containing stimuli-responsive components such as DL-HMPMA or DMAEMA are significantly different from those detected in "ordinary" polymer or copolymer films. To understand the origin of these transitions, we prepared a series of compositionally different p(DMAEMA/nBA) copolymers in the form of colloidal particles that were allowed to coalesce to solid continuous films, and we examined the relationship between the copolymer composition and the new endothermic transitions.

Experimental Section

2-(*N*,*N*-dimethylamino)ethyl methacrylate (DMAEMA) was purchased from Polysciences. Hexadecyltrimethylammonium chloride (HTAC) solution was purchased from Fluka Chemical. 2,2′-Azobisisobutyronitile (AIBN), *n*-butyl acrylate (nBA), and methyl methacrylate (MMA) were purchased from Aldrich Chemical.

p(DMAEMA/nBA) copolymers were synthesized by varying the monomer feed ratio using the semicontinuous emulsion polymerization process outlined elsewhere,[4] which was adapted for a small scale polymerization. The reaction flask was immersed in a water bath preheated to 75 °C and purged continuously with N_2 gas. The reactor was first charged with 27 mL of double-dionized (DDI) water, and after N_2 was purged for 30 min, the content was stirred at 300 rpm. At this point, the pre-emulsion (DDI, HTAC, weight-rationed monomers, and oil-soluble initiator AIBN) was fed at 0.155 mL/min into the vessel over a period of 3 h. After the pre-emulsion feeding was completed, the reaction was continued for an additional 3 h. The resulting colloidal dispersion was filtered after cooling to ambient temperature, and the pH value and the particle size of this colloidal dispersion were approximately pH 8 and 148 nm, respectively, determined by potentiometric titration and light scattering experiments. For comparison, p(nBA), p(DMAEMA), and p(MMA/nBA) were prepared using the same method. In an effort to establish copolymer chemical composition resulting from the synthesis of DMAEMA and nBA monomers, IR and ^{1}H NMR analyses were performed. Figure S-1a, traces A, B, and C, in the Supporting Information illustrates ATR FT-IR spectra of p(nBA) and p(DMAEMA) homopolymers and p(DMAEMA/nBA) copolymer, respectively. Figure S-1b in the Supporting Information provides ^{1}H NMR analysis of the p(DMAEMA/nBA) copolymer.

Molecular weight was determined using gel permeation chromatography (Waters) equipped with a 515 HPLC pump and a 2414 model refractive index detector. Each sample was precipitated in tetrahydrofuran (THF) and eluted through a 5 *μ*m mixed-C column. Elution times were referenced against a polystyrene standard, and molecular weights of p(MMA/nBA) and p(DMAEMA/nBA) copolymers with different DMAEMA/nBA feed ratios were within the 200 000−245 000 g/mol range.

Morphologies of colloidal particles were determined using a Zeiss EM 109-transmission electron microscope (TEM) in which colloidal dispersions were diluted to a 20:1 volume ratio and deposited on a Formvar-coated copper TEM grid (Ted Pella).

* To whom correspondence should be addressed. E-mail: marek.urban@usm.edu. Fax: 601-266-6178.

10.1021/ma802201k CCC: $40.75
Published on Web 02/24/2009

Solid-state NMR CP/MAS spectra were acquired using a UNITY INOVA 400 spectrometer equipped with a Chemagnetics 7.5 mm two-channel solids probe. Samples were spun at a rate of 4.0 kHz. The ^{1}H 90° pulse duration was 5.5 μs and the contact pulse width was 1 ms at 45 ms acquisition time. A proton decoupling field strength of 52 kHz was used to remove ^{13}C−^{1}H dipolar broadening. The free induction decays (FIDs) were zero-filled to 32 K data points, the first four data points were replaced via linear prediction, and Lorentzian and Gaussian apodization was applied prior to Fourier transformation.

We prepared polymeric films by casting colloidal dispersions onto the poly(tetrafluoroethylene) (PTFE) substrate and allowing them to coalescence at 65% relative humidity (RH) for 72 h at 22 °C in an environmental chamber. In a typical experiment, ∼200 μm thick films were obtained. Differential scanning calorimetry (DSC) measurements were performed on a TA Instruments DSC Q 100 using a scanning rate of 5 °C/min from −50 to 70 °C under a N_2 atmosphere. Multiple DSC thermal cycles were conducted using the following heating−cooling schedule: the p(DMAEMA/nBA) specimen was equilibrated at −50 °C for 5 min, followed by heating at 5 °C/min to 70 °C, equilibrating at 70 °C for 5 min, and cooling down at 5 °C/min to −50 °C. The same cycle was repeated several times. The resulting data were analyzed using TA Universal Analysis software. Dynamic mechanical analysis (DMA) measurements were conducted on a TA instruments DMA Q 800. The 20 × 5.6 mm sized films with thickness of ∼200 μm were utilized in the tensile mode, operating at a frequency of 1 Hz and a heating rate of 1 °C/min from −50 to 150 °C.

Thermogravimetric analysis (TGA) measurements were performed on a TA Instruments TGA Q500 to determine the amount of water in coalesced copolymer films. Approximately 20 mg samples were loaded in the platinum pan and heated at 10 °C/min from 25 to 500 °C under a nitrogen atmosphere. The nitrogen flow rate in the balance chamber and furnace was 60 mL/min. For all specimens, the water contained was less than 1.5 ± 0.1% w/w.

Quantum mechanical semiempirical calculations were conducted using Material Studio software (Accelrys Inc., version 4.1). Computer modeling simulations were performed using a classical (Newtonian) molecular dynamics theory combined with the COMPASS force-field conditions. In the first step, we created infinite polymer long chains containing DMAEMA and nBA monomer units using 3D periodic boundary conditions such that the local thermoinduced flux was set to be proportional to the local atom density changes and local thermodynamic driving forces of the chemical potential. In an effort to determine thermodynamic responses of molecular segments, a 23 × 23 × 23 Å^3 periodic unit cell containing 5 polymer chains and 1185 atoms (1185 asymmetric units) was constructed, and temperature was the control parameter to simulate the heat exchange with the environment. This method involves computing NVT (constant number, volume, and temperature) molecular dynamics at a set temperature using 25 000 steps and 25 ps (dynamic times), followed by NPT (constant number, pressure, and temperature) molecular dynamics with 50 000 steps and dynamic times of 50 ps and then NVE (constant number, volume, and energy) molecular dynamics with 100 000 steps and 100 ps. The purpose of this three-step process is to determine energy, volume, and conformational changes theoretically as a function of temperature.

Results and Discussion

The first step in these studies was to compare thermal behaviors of copolymer films. Figure 1a,b illustrates DSC thermograms of p(MMA/nBA) and p(DMAEMA/nBA) copolymer films (water content <1.5% w/w regardless of composition), respectively. Unlike non-stimuli-responsive p(MMA/nBA) copolymer (Figure 1a), which exhibits a single glass transition (T_g) at 6 °C (onset) with mid- and end points at 18 and 31.5 °C, respectively, additional endothermic transition in Figure 1b is detected for p(DMAEMA/nBA) copolymer solid films. As anticipated, the lower transition at −18 °C (onset), with mid- and end points at −10 and 6 °C, respectively, corresponds to the T_g of the copolymer; another endothermic transition at 32 °C is observed, which will be discussed in detail later on. Whereas the 32 °C transition labeled as T_{SR} results from the stimuli-responsive component of the copolymer, a small exothermic increase is detected just before the endothermic transition. This is likely attributed to the increase in free volume with the increasing temperature, which competes with the endothermic polymer chain collapse of the stimuli-responsive components. If this is the case, then colloidal particles should also exhibit heterogeneous morphologies. Indeed, the comparison of the TEM images of p(nBA) and p(DMAEMA/nBA) shown in Figure 2, a and b clearly indicates that p(DMAEMA/nBA) particles exhibit heterogeneous morphologies attributed to the solubility of monomers. During polymerization, nBA, being more hydrophobic and practically insoluble in water, polymerizes first inside the micelles, whereas DMAEMA, being water soluble, copolymerizes on the surface of pnBA seeds and forms a heterogeneous shell. This nanoscale morphology is also maintained in coalesced films. In an effort to determine copolymer composition in solid films, we measured solid-state ^{13}C NMR spectra as a function of temperature.[5] As shown in Figure 3, a, b, and, the choice of temperatures was dictated by the position of specific thermal relaxations of the p(DMAEMA/nBA) copolymer. In particular, solid-state ^{13}C NMR spectra were collected at 11 °C to assess the chain mobility between the T_g values of p(DMAEMA/nBA) at −18 °C and p(DMAEMA) at 20 °C as well as at 25 °C, which is between the T_g of pure p(DMAEMA) at 20 °C and T_{SR} at 32 °C, and at 65 °C (above T_{SR}). The analysis of the NMR spectra shown in Figure 3, a, b, and illustrates the fact that the resonances due to the nBA component detected at 63.9, 31.1, 19.8, and 14.4 ppm remain constant, whereas the peaks due to DMAEMA at 60.0, 57.4, 43.7, and 17.8 ppm exhibit significant broadening for the spectrum recorded at 11 °C. Because the T_g of pnBA is −46 °C, its mobility remains the same above that temperature, which is reflected in the absence of ^{13}C NMR band broadening. In contrast, the T_g of p(DMAEMA) is ∼20 °C (onset 13 °C), and the mobility of the p(DMAEMA) segments will be diminished at 11 °C, which is manifested by the broadening of the resonances due to these segments. Therefore, the presence of separate p(DMAEMA) and p(nBA) domains is part of the film morphologies and is not detected by DSC measurements. As we recall, particle morphologies before coalescence also exhibit similar morphologies.

To identify molecular changes and dynamics of the p(DMAEMA/nBA) copolymer temperature responses, computer modeling experiments using molecular thermodynamics simulations were employed. For that purpose, we created infinite polymer chains by packing energy-minimized DMAEMA/nBA units into a random sequence under 3D periodic boundary conditions, and energy and volume changes were calculated below and above the T_g and T_{SR} temperatures. Inserts I, II, III, and IV in Figure 1b depict conformational and volume changes at selected temperatures and transitions, whereas the calculated energy and volume values are summarized in Table 1. As seen for the T_g transition, the calculated total energy of the system (ΔE_{tot}), which is comprised of the potential (E_{pot}) and kinetic energies (E_{kin}), increases by 168 kcal/mol (from 2377 to 2545 kcal/mol). At the same time, the E_{pot} values change by 71 kcal/mol (from 1468 to 1539 kcal/mol), whereas E_{kin} increases by 97 kcal/mol (from 909 to 1006 kcal/mol). For the T_{SR} transition, the total energy (ΔE_{tot}) increases by 223 kcal/mol (from 2753 to 2976 kcal/mol), E_{pot} changes by 131 kcal/mol (from 1668 to 1799 kcal/mol), and E_{kin} changes by 92 kcal/mol (from 1084 to 1176 kcal/mol). It should be noted that significantly greater E_{pot} changes were obtained for the T_{SR} compared with the T_g

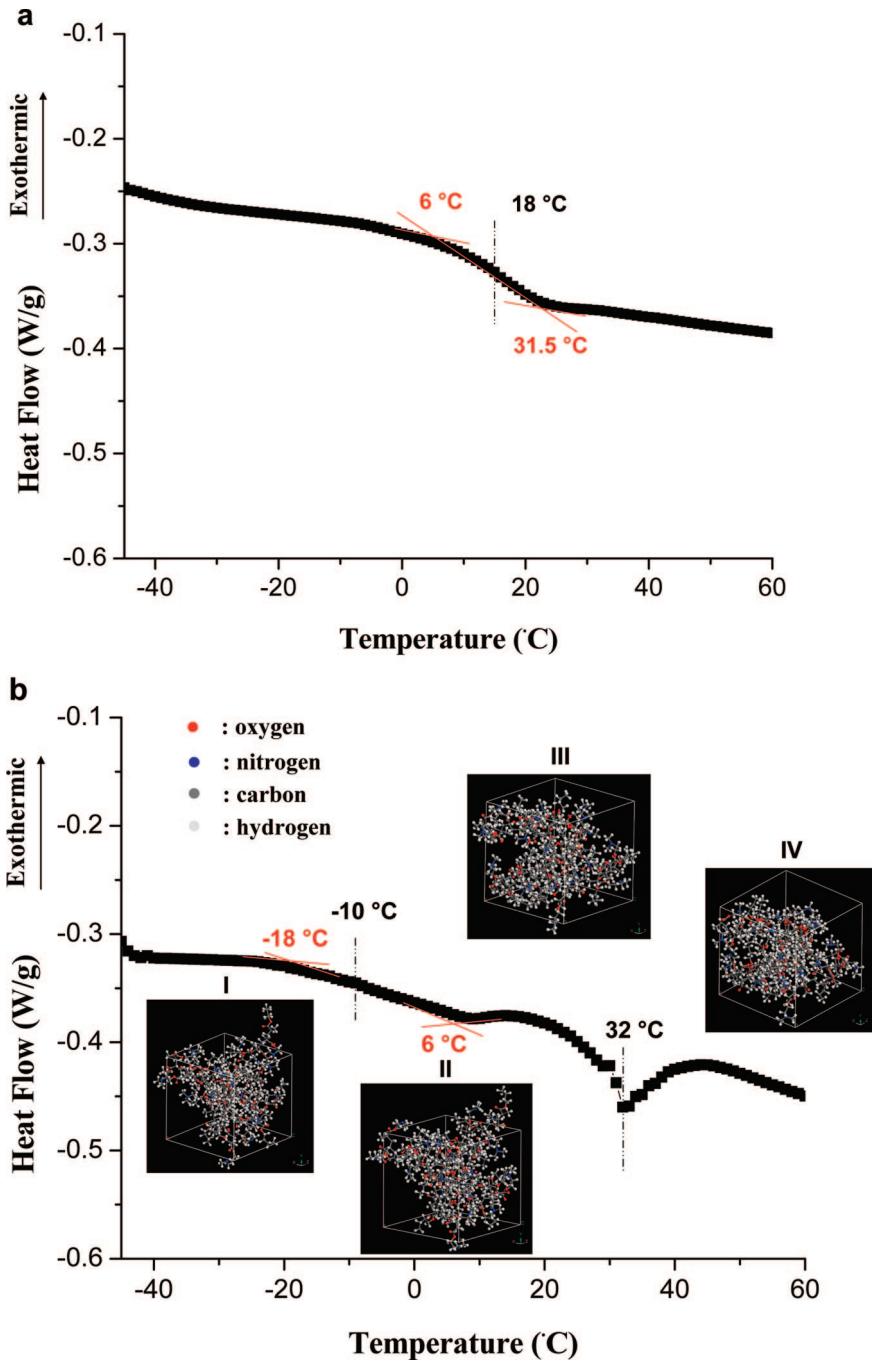

Figure 1. Differential scanning calorimetry (DSC) thermograms of (a) p(MMA/nBA) and (b) p(DMAEMA/nBA) (feed ratio = 1:1) copolymers. Inserts represent the results of the computer simulations and illustrate the volume and conformational changes at: −20 (insert I), 5 (insert II), 25 (insert III), and 45 °C (insert IV).

transitions, which is attributed to larger conformational changes occurring during the T_{SR} transition. For both transitions, the calculated ΔE_{tot} values are in good agreement with the energy values obtained from the DSC experiments, which are 122 kcal/mol for the T_g and 199 kcal/mol for the T_{SR}, and small differences are attributed to the inclusion of the entropic components in ΔE_{tot} calculations. Furthermore, computer simulation experiments also show that as a specimen undergoes the T_{SR} transition, the volume (V) decreases by 21.6% (from 12.15 to 9.52 nm^3) as compared with the 1.7% change (from 10.86 to 11.05 nm^3) for the T_g transition. These results are also depicted in the 3D unit-cell inserts shown in Figure 1b. Table 1 also lists experimentally determined volume changes; above T_{SR}, the volume decreases 29% (from 28.94 to 20.40 nm^3), and these changes are reversible. It should be noted that the kinetics of heating and cooling cycles are not the same, and longer times are required for cooling because of slower chain mobility.

In an effort to determine how DMA measurements are sensitive to the presence of the T_{SR} transitions, we collected DMA data on the same specimens. As shown in Figure 4a,b, the T_g transitions of p(MMA/nBA) and p(DMAEMA/nBA) represented by two maxima in the tan δ curves (curves A and A′, respectively) are detected at 17 and −12 °C, respectively. These data are in agreement with the DSC measurements. Furthermore, the storage modulus (E') of p(DMAEMA/nBA) copolymer films (curve B′) begins to increase at 31 °C. This is attributed to the shrinkage of p(DMAEMA/nBA) films and the collapse of the copolymer backbone. As the film density

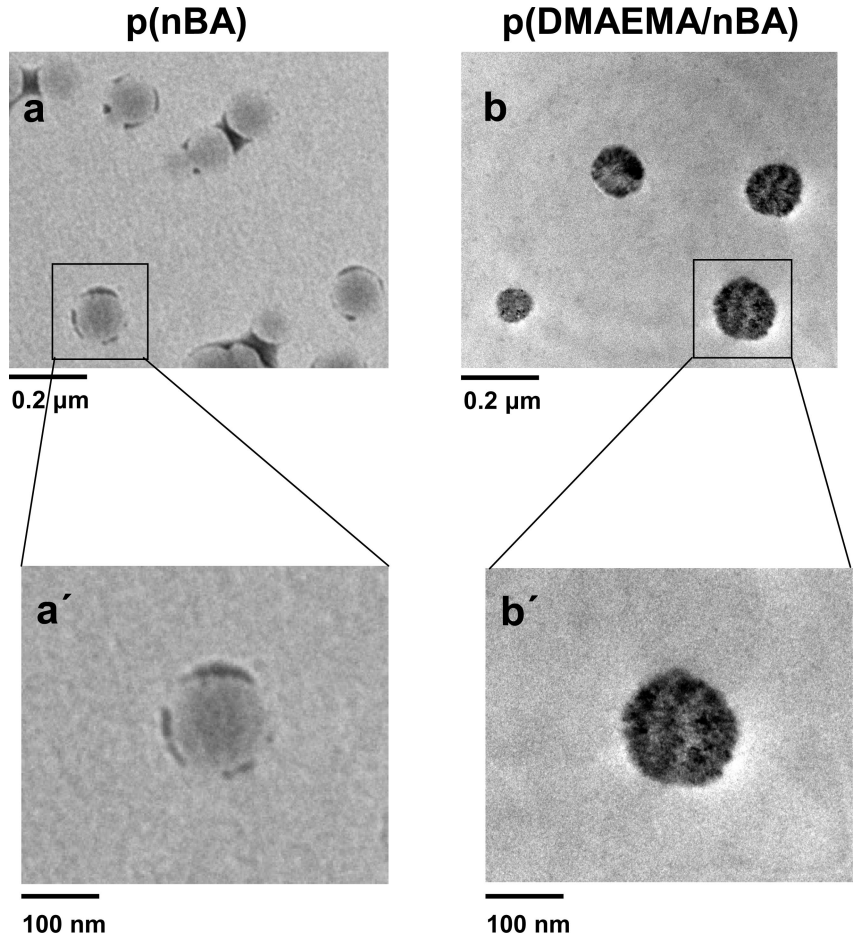

Figure 2. TEM images of p(nBA) and p(DMAEMA/nBA) (feed ratio = 1:1) colloidal particles.

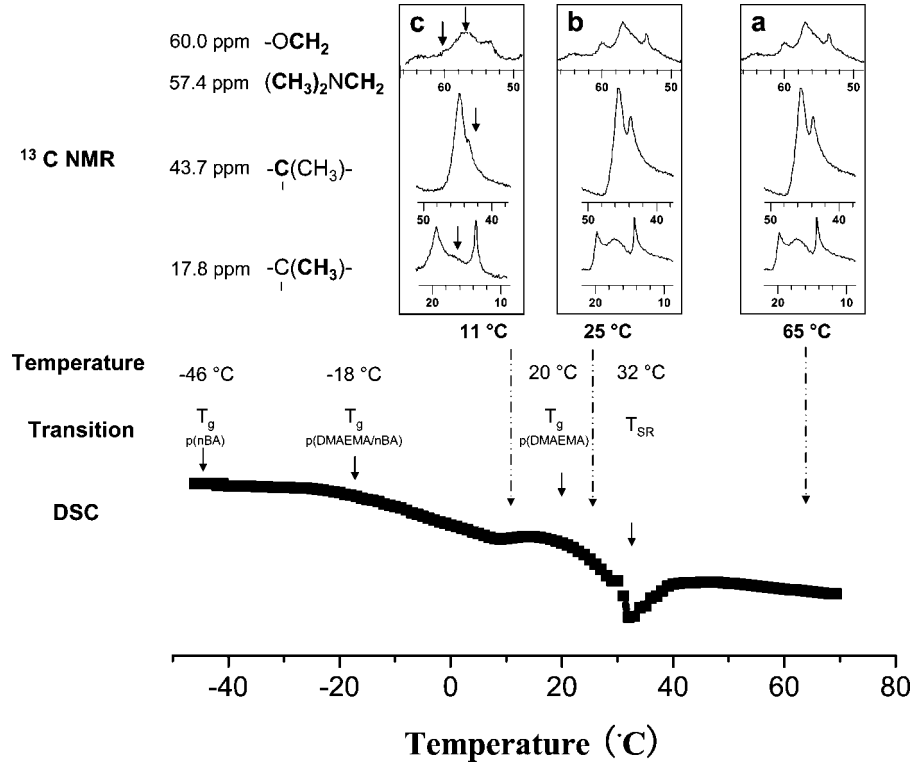

Figure 3. Solid-state ^{13}C NMR spectra of p(DMAEMA/nBA) (feed ratio = 1:1) films conducted at 11, 25, and 65 °C. For comparison, DSC curve is included.

Table 1. Computer Simulation Results of Energy and Volume Changes

		total energy (kcal/mol)	ΔE_{tot} (kcal/mol)	potential energy (kcal/mol)	ΔE_{pot} (kcal/mol)	kinetic energy (kcal/mol)	ΔE_{kin} (kcal/mol)	volume theor (nm^3)	ΔV_{theor} (nm^3)	volume exptl (mm^3)	ΔV_{exptl} (mm^3)
T_g	−20 °C	2377	↑ 168	1468	↑ 71	909	↑ 97	10.86	↑ 0.19		
	5 °C	2545		1539		1006		11.05			
T_{SR}	25 °C	2753	↑ 223	1668	↑ 131	1084	↑ 92	12.15	↓ 2.63	28.94	↓ 8.54
	45 °C	2976		1799		1176		9.52		20.40	

increases, mechanical strength is enhanced. In contrast, the E' values for p(MMA/nBA) (curve B) show expected glassy and rubbery plateaus. The loss moduli (curves C and C′) for both copolymer films are similar. It should be noted that the energy changes at the T_{SR} transition shown in the DSC curves are significantly stronger than the storage modulus changes detected by DMA. These observations suggest that for T_{SR} to occur a certain amount of thermal energy must be employed for polymer chains to collapse and adapt to new conformation changes, but insignificant segmental motion changes are anticipated. As a result, the magnitude of these transitions in DSC is significant, but the same transitions in DMA measurements are not as pronounced.

Whereas the above discussion focused on the T_{SR} transition in p(DMAEMA/nBA) films with a feed ratio of 1:1 DMAEMA/nBA, the main question is whether and how the changes of the DMAEMA/nBA copolymer ratio will affect the T_{SR} transitions in solid films. Figure 5 illustrates a series of DSC thermograms of p(DMAEMA/nBA) copolymer films recorded for different DMAEMA/nBA copolymer compositions. As seen, similar to copolymer composition-dependent T_g transitions, the T_{SR} transitions also shift to higher temperatures as the amount of the stimuli-responsive DMAEMA component increases in the DMAEMA/nBA copolymer. For p(DMAEMA) homopolymer, the DSC data show also two transitions: the onset T_g at 13 °C with the midpoint at 20 °C and the T_{SR} at 40 °C. The literature reported midpoint T_g values for this homopolymer are in the 16−24 °C range.[6]

If the T_{SR} relaxation is indeed responsible for the stimuli-responsive component, one would anticipate it to be reversible. Figure 6 illustrates the DSC heating−cooling cycles for p(DMAEMA/nBA) 1:1 copolymer ratio. As observed, upon the first heating cycle, T_g and T_{SR} are detected, but upon cooling, only T_g is present. In the second heating cycle, exactly the same DSC response with two transitions is detected. This process was repeated many times, and the T_{SR} transition is not detectable upon cooling because the system requires longer times for chain

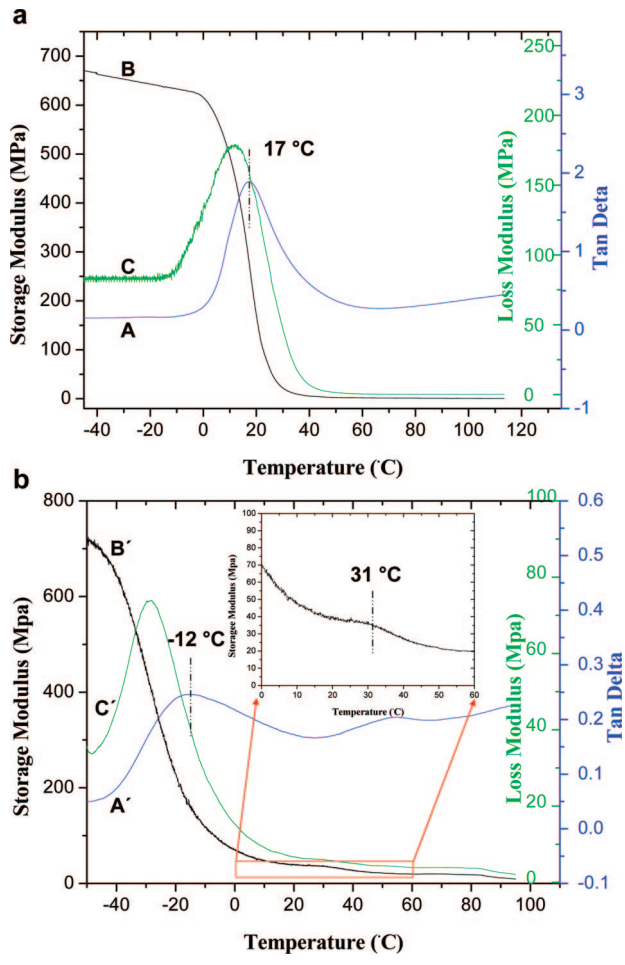

Figure 4. Dynamic mechanical analysis (DMA) results of (a) p(MMA/nBA) and (b) p(DMAEMA/nBA) (feed ratio = 1:1) copolymer films: plots A and A′, tan δ; plots B and B′, storage modulus (E'); and plots C and C′, loss modulus (E'') for each copolymer, respectively.

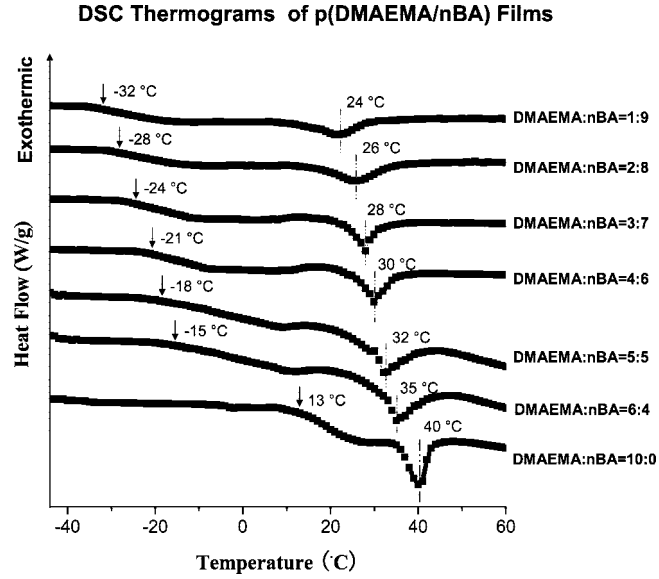

Figure 5. Series DSC thermograms of p(DMAEMA/nBA) copolymer films recorded for different DMAEMA/nBA weight ratios.

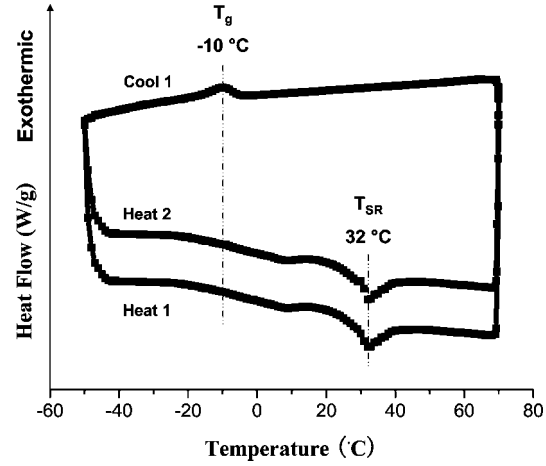

Figure 6. Multiple DSC cycles conducted on p(DMAEMA/nBA) copolymer.

expansions. This behavior was also reflected in slower response to the volume changes upon cooling (Table 1). It takes about 24 h to reach the initial equilibrium state.

With these data in mind it is appropriate to relate the T_g, T_{LCST}, and T_{SR} transitions and realize that these transitions were detected for solid continuous films that contain only traces of water (1.5 ± 0.1% w/w). Although one could anticipate that these amounts of water could be responsible for localized two-phase water−polymer interactions and thus potentially be responsible for the observed T_{SR} endothermic transitions, this is not the case. If the T_{SR} shift as a function of copolymer composition was attributed to the water content, then the amount of water would parallel the copolymer composition changes. It should be pointed out that the T_{LCST} observed in aqueous polymeric solutions is manifested by the particle size decrease above T_{LCST} due to demixing behavior.[7] For colloidal particles composed of only p(DMAEMA) (no nBA present in copolymerization), LCST/demixing behavior in water occurs, which is well documented in the literature for similar dispersions.[3,8,9] Because these experiments were conducted on solid continuous films, the presence of a stimuli-responsive component such as DMAEMA results in endothermic T_{SR} transitions. For p(DMAEMA) homopolymer, the value of T_{SR} is equal to the temperature of a binary polymer−water (p(DMAEMA)−water) system (T_{binary}), which is the temperature at which the polymer−water system phase separates into a water and a polymer phase. Also, for p(DMAEMA) homopolymer, the values of T_{SR} and T_{binary} may be numerically equal, but the physical meaning is different. T_{binary} results from the phase separation at the temperature−concentration diagrams with the minimum corresponding to T_{LCST}. Although extensive data available for homopolymer, copolymer, microgels, or hydrogels[10−16] are associated with the polymer−water phase behavior, these mechanically stable coalesced films exhibit composition-dependent T_g and T_{SR} transitions, the latter being manifested by the conformational changes that are responsible for the overall film volume changes.

In an effort to relate T_{SR} and T_{binary}, the relationship that allows us to predict the T_{SR} values as a function of copolymer composition was established

$$\frac{1}{T_{SR}} = \frac{w_1}{T_{binary}} + \frac{w_2}{T} \quad \text{or} \quad \frac{1}{T_{SR}} = w_1\left(\frac{1}{T_{binary}} - \frac{1}{T}\right) + \frac{1}{T} \qquad (1)$$

where w_1 is the weight fraction of stimuli-responsive monomer 1, w_2 is the weight fraction of non-stimuli-responsive monomer 2 ($w_2 = 1 - w_1$), T_{binary} is the temperature of stimuli-responsive p(DMAEMA) homopolymer in a binary polymer−water equilibrium (313 K)[3] with the minimum at the temperature−concentration diagrams corresponding to T_{LCST}, and T is the film-formation temperature. The same form exhibits the Fox equation for predicting the T_g changes with the composition of the copolymers. For comparison, Figure 7a,b illustrates the relationship between T_g and T_{SR} as a function of w_1, respectively. The T_g and T_{SR} changes as a function of composition exhibit similar trends, but their magnitude is different. The T_g changes as a function of composition are independent of the stimuli-responsive component, and if the former is substituted by a non-stimuli-responsive monomer like MMA, then no T_{SR} transitions are detected in DSC and DMA measurements, as illustrated in Figures 1 and 4.

To determine the validity of eq 1, we compared the experimental T_{SR} values obtained from DSC measurements with the calculated values obtained from eq 1 and plotted them in Figure 8. The solid cubic (■) points represent the DSC experimental data points, and lines a−k represent predicted T_{SR} value changes as a function of w_1 for different T values. It should be noted that when $w_2 = 0$, $1/T_{SR} = 1/T_{binary}$, and thus T_{SR} is 313 K. Extrapolation of $w_1 \rightarrow 0$ has no physical meaning because the T_{SR} transitions do not exist because there is no stimuli-responsive monomer copolymerized into the copolymer. It should also be noted that lines a and b in Figure 8 corresponding to $T = 298$ and 296 K, respectively, exhibit the best fit with the experimental data points within ±0.61 and ±0.22, respectively.

To justify the significance of the above relationship further, eq 1 was used to determine T_{binary} and T values from experi-

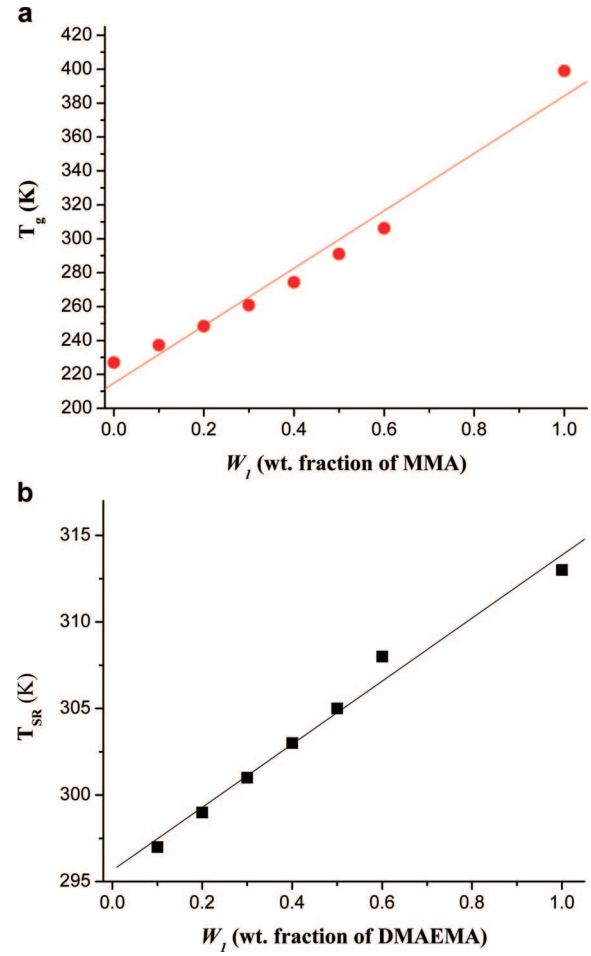

Figure 7. (a) T_g and (b) T_{SR} plotted as a function of w_1.

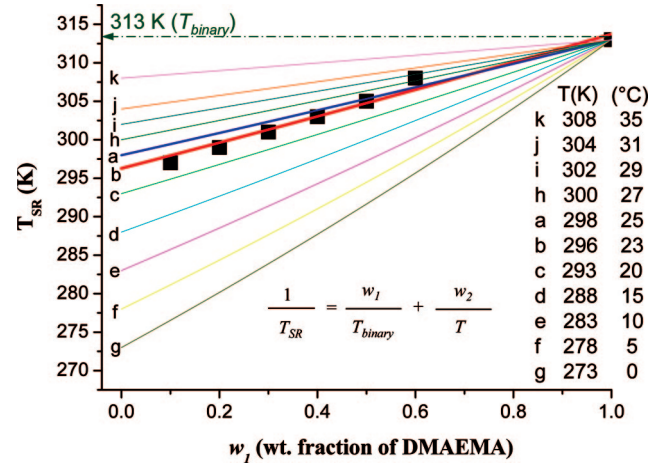

Figure 8. Experimental T_{SR} values obtained from DSC measurements and predicted T_{SR} using eq 1 for different T values plotted as a function of w_1.

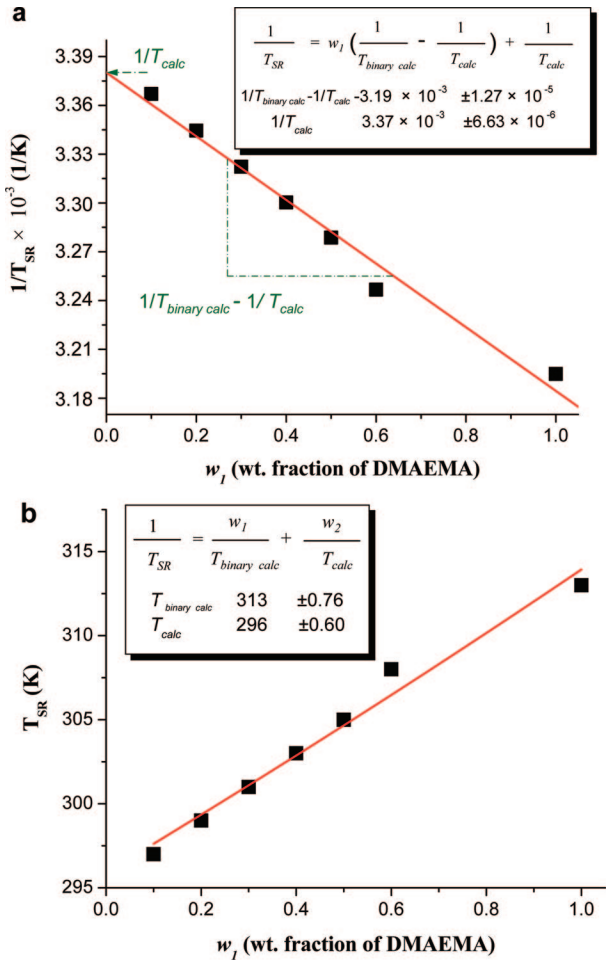

Figure 9. Curve fitting of experimental T_{SR} data obtained from DSC measurements with eq 1: (a) $1/T_{SR}$ versus w_1 and (b) T_{SR} versus w_1.

mental DSC measurements using detected T_{SR} transitions and weight fractions of each monomer w_1 and w_2. Figure 9a illustrates a plot of $1/T_{SR}$ versus w_1, with the slope equal to $1/T_{\text{binary calc}} - 1/T_{\text{calc}}$ and an intercept of $1/T_{\text{calcd}}$. To illustrate the direct relationship, the T_{SR} versus w_1 plot shown in Figure 9b was also constructed. As seen, the calculated $T_{\text{binary calc}}$ and T_{calc} correspond exactly to the values of T_{binary} of the p(DMAEMA) homopolymer at 313 K and a given T at 296 K.

Conclusions

These studies show for the first time the presence of new thermal transitions of stimuli-responsive p(DMAEMA/nBA) copolymer films. Unlike in the solution phase, where LCST transition is easily attainable because Brownian motion of surrounding solvent molecules requires relatively low energy and shorter times for macromolecular segments to displace, solid copolymers require the design of copolymer segments that are capable of rearranging and maintaining solid-state properties. This was accomplished by copolymerizing low-T_g, high-free-volume, stimuli-responsive monomers. As shown in DSC and DMA measurements, relaxations detected experimentally in stimuli-responsive copolymers in the form of T_{SR} transitions are in agreement with theoretical computer simulations. On the basis of the experimental data, the relationship $1/T_{SR} = w_1/T_{\text{binary}} + w_2/T$ was established to predict the T_{SR} values as a function of copolymer composition and temperature.

Acknowledgment. This work was primarily supported by the MRSEC Program of the National Science Foundation under award no. DMR 0213883 and partially supported by the DMR 0215873 Major Research Instrumental (MRI) Program. We are grateful to Dr. W. Jarrett for his help in conducting NMR experiments and Professor Kris Matyjaszewski for his useful suggestions.

Supporting Information Available: ATR FT-IR spectra of p(DMAEMA), p(nBA), and p(DMAEMA/nBA) and ^{1}H NMR spectrum of p(DMAEMA/nBA) in DMSO This material is available free of charge via the Internet at http://pubs.acs.org.

References and Notes

(1) Liu, F.; Urban, M. W. *Macromolecules* **2008**, *41*, 352.
(2) Misra, A.; Jarrett, W.; Urban, M. W. *Macromolecules* **2007**, *40*, 6190.
(3) Liu, F.; Urban, M. W. *Macromolecules* **2008**, *41*, 6531.
(4) Lestage, D.; Urban, M. W. *Langmuir* **2005**, *21*, 2150.
(5) Koenig, J. L. *Spectroscopy of Polymers*; American Chemical Society: Washington, DC, 1992.
(6) Tobolsky, A. V.; Shen, M. C. *J. Phys. Chem.* **1963**, *67*, 1886.
(7) Gil, E. S.; Hudson, S. M. *Prog. Polym. Sci.* **2004**, *29*, 1173.
(8) Okubo, M.; Ahmad, H.; Suzuki, T. *Colloid Polym. Sci.* **1998**, *276*, 470.
(9) Burillo, G.; Bucio, E.; Arenas, E.; Lopez, G. *Macromol. Mater. Eng.* **2007**, *292*, 214.
(10) Pelton, R. H. *Colloids Surf., B* **1986**, *20*, 247.
(11) Pelton, R. H. *Adv. Colloid Interface Sci.* **2000**, *85*, 1.
(12) Aoki, T.; Murematsu, M.; Nishina, A.; Sanui, K.; Ogata, N. *Macromol. Biosci.* **2004**, *4*, 943.
(13) Aoki, T.; Muremamatsu, M.; Torii, T.; Sanui, K.; Ogata, N. *Macromolecules* **2001**, *34*, 3118.
(14) Yuk, S. H.; Cho, S. H.; Lee, S. H. *Macromolecules* **1997**, *30*, 6856.
(15) Heijl, J. M. D.; Prez, F. E. D. *Polymer* **2004**, *2004*, 6771.
(16) Xu, F.-J.; Kang, E.-T.; Neoh, K.-G. *Biomaterials* **2006**, *27*, 2787.

MA802201K